五百米口径球面射电望远镜脉冲星研讨会(9)

FAST Pulsar Symposium 9

https://psr.pku.edu.cn/fps/FPS9/FPS9.html

Local organizers

Huiqing Hong (XMU)
Jinchen Jiang (PKU)
Ang Li (XMU, Chair)
Tong Liu (XMU)
Jiguang Lu (NAOC)
Fang Luo (XMU)
Xingyu Shao (XMU)

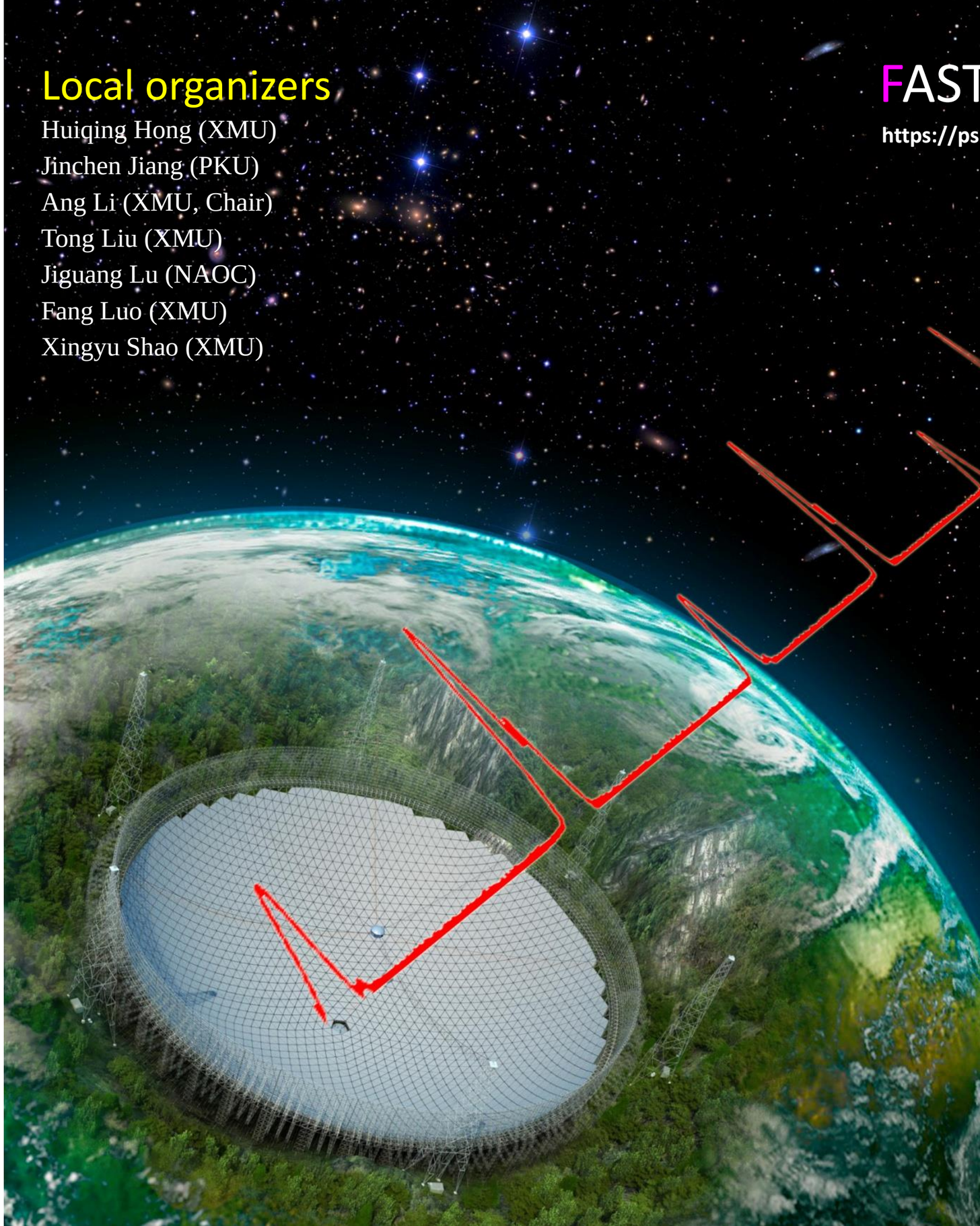

Xiamen University
Xiamen
August 28-30, 2020

Organized by FPS Advisory Committee

Hsiang-Kuang Chang (NTHU)
Longfei Hao (YNO)
Stephen Ng (HKU)
Hongguang Wang (GZU)
Jianping Yuan (XAO)
Youling Yue (NAO)
Li Zhang (YNU)
Biping Gong (HUST)
Yongfeng Huang (NJU)
Liming Song (IHEP)
Renxin Xu (PKU)
Yefei Yuan (USTC)
Zhen Yan (SHAO)
Xiaoping Zheng (CCNU)


FAST / Future Pulsar symposium 9
2020.08.28-30 Xiamen

500 米口径球面射电望远镜/未来脉冲星专题研讨会

第九次会议

受“973 计划”项目资助而发起、组织的 FPS 年会承载着“脉冲星人才培养”之重任。因新冠疫情，2020 年 FPS 会议推迟至 8 月 28 日至 30 日在厦门成功线下举办。FPS9 评奖委员会（戴子高、龚碧平、黄永锋、来小禹、李昂、李茁、李柯伽、李兆升、刘彤、邵立晶、仝号、童明雷、王洪光、魏薇、徐仁新、朱炜玮、张彬彬、张洁、郑小平等 19 人构成）最终遴选出 Crab 奖一名（姚菊梅）、Vela 奖三名（高勇、门云鹏、张蕾）。很遗憾忘了拍摄四位获奖者的现场合影（**今后得记住**），只得将与颁奖者的合影呈现于此。

FPS9 获奖者及颁奖者

姚菊梅/戴子高 高勇/郑小平 门云鹏/李茁 张蕾/徐仁新

与会者，无论是做理论的（“取诸怀抱，悟言一室之内*”）还是做观测的（“因寄所托，放浪形骸之外*”），大家在此齐聚一堂、阐心得明志趣。相信又一年的 FPS 集会再次激发少长学人索求真理的无尽热情，而免“及其所之既倦，情随事迁*”之忧！

作为“FPS 人”共同的“历史记忆”，您手中是第九本会议文集。相信文集在会场外将进一步绽放 FPS 的精神魅力、熏陶一代又一代“脉冲星”学子... 已有 FPS 文集电子版网址如下：

https://psr.pku.edu.cn/fps/Proceedings/ FPSα.pdf

这里α= 1,2,3,…9，代表获取第一到九次的 FPS 文集。作者们风格独特、构思巧妙，相信读者们定能觅见自己欣赏、口味相投的作品；这将为进一步的沟通交流提供桥梁。

会议组委者：“FPS”咨询委员会

厦门大学 洪惠卿、李昂（主席）、刘彤、罗芳、邵星宇

国家天文台 卢吉光，北京大学 姜金辰

公元贰零贰零年拾贰月

*取自魏晋时期王羲之（303 年生， 361 年卒）散文《兰亭集序》。

目 录

中子星的超流性与冷却

董建敏 (Renxin Xu)
中科院近代物理研究所
兰州 730000
Email: dongjm07@impcas.ac.cn

中子星冷却是天体物理和核物理共同关注的重要研究领域。随着天文观测数据大量的积累和精度的提高， 人们期望通过观测来提取中子星 结构以及高密度核物质的一些基本信息。特别是，天文观测上Cas A超新星遗迹中子星的快速冷却的发现，不仅激发了人们对中子星冷却本身的极大兴趣，同时也推动了人们对核物质超流性和中微子发射等重要问题的研究。 另外，核子之间短程关联是当前核物理研究中备受关注的一个重要问题， 对于核结构、核物质的一些性质以及重离子反应的研究都有非常重要的意义。

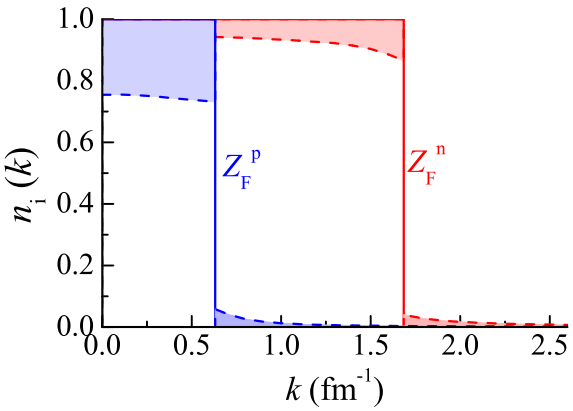

Figure 1: 核子动量分布示意图

首先研究了纯中子物质中由于费米面偏离自由费米气体中费米分布导致的对$^3PF_2$ 态超流性的影响（即Z-因子效应，如图1所示）。当不考虑Z-因子效应时，中子物质中3PF2态超流性可以存在于很宽的密度范围，对能隙较大。 Z-因子效应将强烈抑制中子物质中$^3PF_2$态超流性，导致对能隙压低一个量级。考虑Z-因子效应后，能隙的峰值被压低到0.05 MeV。结果对于$^3PF_2$超流性在中子星冷却中所起的作用提出了疑问。进一步，将计算推广到一般同位旋非对称核物质及beta稳定物质， 并计算了由于费米面排空效应对中子星冷却过程其它输入量的影响，包括中微子发射、 物质热容量等。在此基础上，进一步给出了费米面排空效应对冷却曲线的影响，如图2所示。 研究结果表明：1）费米面排空效应会导致中子星物质中超流能隙压低一个数量级， 从而对超流性在中子星冷却中的作用提出了质疑。

2）费米面排空效应并不能改变直接Urca过程的阈值； 如果直接Urca过程能够发生，费米面排空效应将导致中微子发生率的降低， 该结论与人们以往的预期完全相反。此外，间接Urca过程、韧致辐射和$^3PF_2$库珀对形成-破缺过程的中微子发射率也被压低， 而且这一压低效应在高密度情况下尤为明显。 3）中子星内部 β 稳定物质热容量被降低。4）年轻中子星的冷却会被延缓，因此，在精确研究中子星热演化时， 费米面排空效应需要被考虑。这项研究澄清了核子短程关联导致的高动量尾巴在中子星冷却中的作用，对于中子星冷却和核子短程关联的研究都具有一定的参考意义。

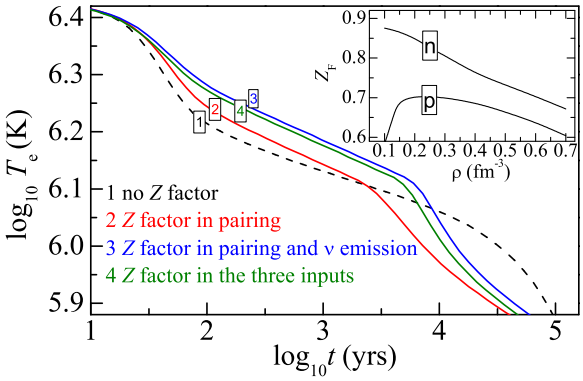

Figure 2: 费米面排空效应对中子星冷却的影响

J. M. Dong, U. Lombardo, & W. Zuo, 2013, PhRvC, 87, 062801(R).
J. M. Dong, U. Lombardo, H. F. Zhang, & W. Zuo, 2016, ApJ, 817, 6.
J. M. Dong, L. J. Wang, & W. Zuo, 2018, ApJ, 862, 67.

自由进动中子星：电磁和连续引力波辐射

高勇 (Yong Gao)，Vela奖获得者
北京大学物理学院天文学系
北京 100871
Email: gaoyong.physics@pku.edu.cn

一颗自由进动的中子星会调制脉冲星的射电信号并且产生连续引力波。对这种运动的研究与搜寻，对研究中子星壳层，内部磁场强度及位形和内部超流等有重要的启示。中子星产生自由进动的条件有两个：一是有非转动引起的形变，二是瞬时转动轴和角动量不重合。形变的来源主要有固态壳层中的弹性形变和中子星内部各向异性的强磁场。我们用$\epsilon = (I_3 - I_1)/I_1$来表征形变的程度，其中$I_1$和$I_3$是沿着惯量主轴的最小和最大的转动惯量。中子星非常致密，无论是弹性形变储存的弹性能还是内部各向异性磁场具有的能量相对于引力能都非常小的，所以形变参数ϵ非常小（$\sim 10^{-7}$或者更低）[1]。粗略来看，自由进动可以分解为绕着角动量的转动（通常所说的中子星的自转）和中子星本身绕着其中一个惯量主轴的转动（本文所说的进动）。进动周期$P_{\rm p}$和转动周期$P_{\rm r}$之间的关系是$P_{\rm p} \sim P_{\rm r}/\epsilon$，由于形变量很小，进动比转动慢很多。

自由进动在射电辐射中具有可观测的效应：磁轴固着在中子星上，所以中子星的磁轴一边绕着角动量的方向做转动，一边绕着一个惯量主轴做慢速的进动。进动会改变辐射区相对于转动轴的倾角，也会对脉冲到达时间有一个周期性的调制。如果我们观测到了自由进动，就可以对脉冲星的辐射模型，磁倾角等物理量提供重要的信息。另一方面，做自由进动时质量四极矩会发生改变，会辐射引力波。频域上来看，引力波主要集中在转动频率和两倍转动频率处。引力波的观测，能为我们提供更多中子星内部结构的信息。

目前，LIGO和Virgo等探测器正在搜寻形变中子星形变产生的连续引力波，而FAST也有可能在将来搜寻到来自进动调制的射电信号。引力波和电磁波对进动中子星的多信使观测，有可能对中子星内部结构和物态给出重要的信息。

[1]打个比方，相当于一颗10 km的中子星只有1 mm甚至更低的形变量。探测这种形变也就具有很大的挑战性。

Periodic and Phase-locked Modulation in The MP and IP of PSR B1929+10

寇菲菲 *(Feifei Kou)*
中国科学院国家天文台
北京 *100101*
Email: koufeifei@xao.ac.cn

We present a detailed single-pulse analysis for PSR B1929+10 based on observations with the Five-hundred-meter Aperture Spherical radio Telescope (FAST). The main pulse and interpulse are found to be modulated with a periodicity of ~ 12 times the pulsar's rotational period (P). The $\sim 12P$ modulation is confirmed as a periodic amplitude modulation instead of systematic drifting, because there is no systematic drifting features detected in our data.

The longitude-longitude correlation between the MP (from -57° to 34°) and the IP (from 164° to 210°) at zero delay is shown in the left panel of Fig. 1. The region is largely negative for the correlation (blue) between the IP and the weak preceding component of the MP, but weakly positive (red) for the correlation between the IP and the first two components of the MP. This means that the emission in IP is anti-correlated with that of the weak preceding component of the MP, but correlated with that of the first two components of the MP. The correlation diagram indicates that the pulse longitudes with the same modulation period are locked.According to the correlation diagram, the longitudes of the MP with negative correlation correspond to the weak preceding component (MP_I). The regions with positive correlation correspond to the first two components (from -15° to 2°), and called MP_II. The cross-correlations between the pulse energies of the IP and parts of the MP are shown in the right panel of Fig. 1. It can be seen that the cross-correlation reaches its maximum value of -0.37 at zero lag (the solid line). This means that the pulse energy modulation of the IP is anti-correlated with that of the MP_I, which is called phase-locked modulation. Contrary to the negative correlation between the IP and the MP_I, the energy variation of the IP is positively correlated with that of the MP_II (the dashed line in the right panel of Fig. 1). The peak of the correlation function is about 0.45. We notice that the peak of the correlation function is offset from zero lag, which corresponds to a delay of $\sim 1P$. This is referred to as a phase-locked delay.

The above results are a conundrum for pulsar theories and cannot be satisfactorily explained by the current pulsar models. It is puzzling that the IP and the MP are phase locked. These facts imply that the magneto- sphere should be modulated periodically and globally, and there should be transfer of information between different emission regions or poles. Our results observed with FAST provide an opportunity to probe the structure of pulsar emission and the neutron star's magentosphere.

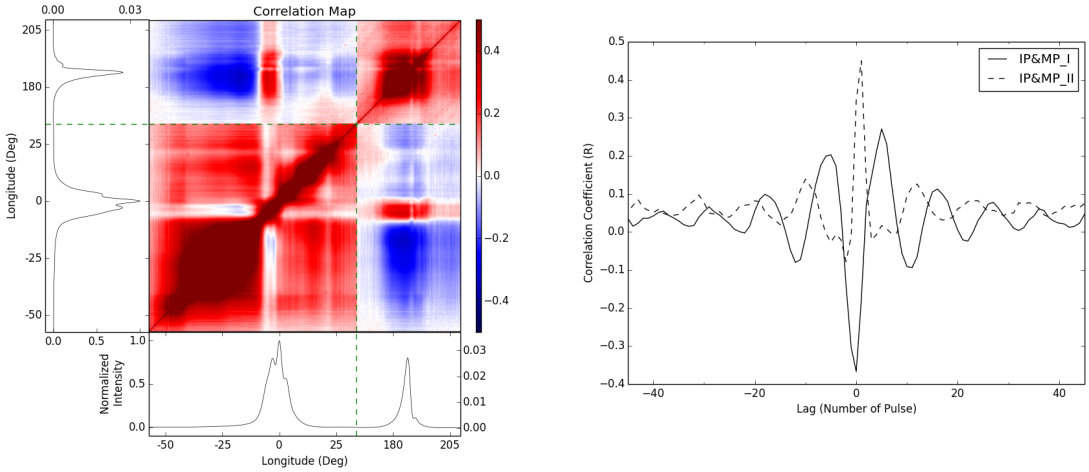

Figure 1: Left:The longitude-longitude correlation between the MP and the IP for zero delay. The side and bottom windows show the mean pulse profile with intensity normalized to the peak of the MP. Right: The cross-correlations between the pulse energies of the IP and other parts of the MP. The solid line is for the IP and the MP_I , and dashed line is for the IP and the MP_II.

The paper has been published in ApJ (`https://iopscience.iop.org/article/10.3847/1538-4357/abd545`).

利用短伽马射线暴晚期射电余辉限制双中子星并合产物

刘良端 *(Liangduan Liu)*
北京师范大学天文系
北京 *100875*
Email: liuliangduan@bnu.edu.cn

2017年8月17日人类首次探测来自双中子星并合引力波 GW 170817和与之在时间上和空间上都成协的短伽马射线暴 GRB 170817A，表明至少有一部分短伽马射线暴来自于双中子星并合[1]。由于人们目前对中子星状态方程的了解还不够，目前还不清楚并合产物是一个黑洞还是一个长期存在的中子星。

数值模拟表明，双中子并合时由于动力学以及盘风的过程，将会产生一部分物质抛射，其典型的质量$M_{\rm ej} \sim 10^{-3} - 10^{-2} M_{\odot}$，典型的速度$v_{\rm ej} \sim 0.1 - 0.3c$。这团抛射物会和暴周环境介质产生相互作用，通过激波加速后电子的同步辐射，在暴后几年后产生射电信号。

如果双中子星并合产物是是一个黑洞，如果没有非常强的吸积过程，它将无法为并合抛射物提供额外的能量，抛射物的动能$E_{\rm K} \sim 10^{49} - 10^{50}$ erg. 而如果并合产物是一个具有强磁场、快速转动的中子星，它将有可能将大部分的转动能转化为抛射物的动能，使得抛射物动能提高两个量级左右，即$E_{\rm K} \sim 10^{52}$ erg.

通常情况下，由相对论性喷流产生的伽马暴射电余辉已经在暴后几百天之后下降到观测极限之下了。在暴后几年这个时标内，由抛射物与环境相互作用产生的射电信号占主导作用。而短暴暴发几年后射电信号的强度非常依赖于抛射物的动能，因此短伽马射线暴晚期射电余辉有助于限制双中子星并合产物。

此前国际上有好几个小组[2, 3]，尝试寻找短伽马暴后几年后的射电信号，到目前为止还没有探测在几年这个时间尺度上与短暴成协的射电信号。这些小组 利用这些零探测的结果排除了某些短暴的中心引擎是一个磁星。 我们发展了一个更加细致的理论模型 [4]，考虑了能量注入的动力学模型、相对论效应与深度非相对论效应的物理过程。我们发现此前过于简化的模型，给出的理论上的射线流量偏高了。导致了他们对磁星存在的参数空间过于严格。 我们的计算结果表明，目前的零探测这个结果，还不足以排除任何一个短暴中心引擎是磁星的可能性。如图1所示，对于GRB 170817A虽然磁星存在的参数空间被压缩在左下方的角落，但是还是不足以将磁星完全排除。

目前这些射电信号零探测得到的观测上限大多在$10 - 100\mu$Jy,而 FAST的观测此类信号的观测灵敏度，有可能达到0.1μJy量级。所以FAST是搜索这类信号的利器，如果真的探测到这样的射电信号，对磁星模型是很大的支持，而如果还是无法探测到这样的信号，对磁场存在参数空间将会进步一压缩。

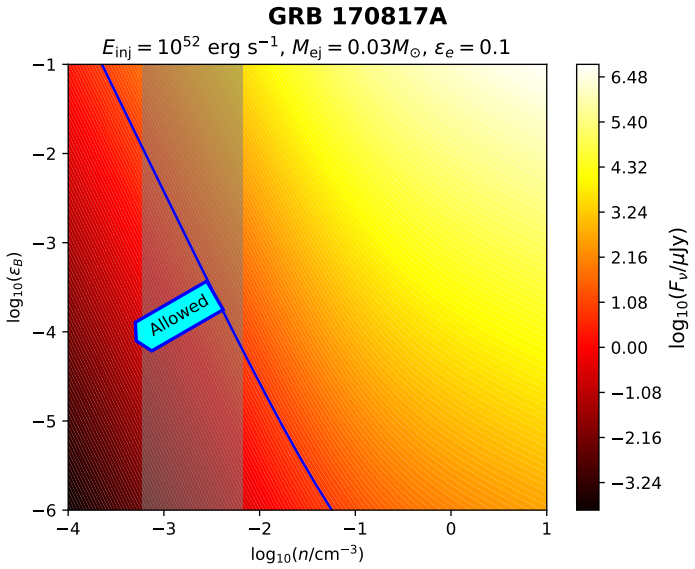

Figure 1: 利用晚期射电观测对GRB 170817A磁星可能存在参数空间的限制。蓝色实线左下方是磁星模型还能允许的范围，垂直的阴影区域表示通过多波段余辉拟合得到的介质密度分布范围。

References

[1] Abbott, B. P., Abbott, R., Abbott, T. D., et al. 2017, ApJL, 848, L13

[2] Metzger, B. D., & Bower, G. C. 2014, MNRAS, 437, 1821

[3] Fong, W., Berger, E., Margutti, R., & Zauderer, B. A. 2015, ApJ, 815, 102

[4] Liu, L.-D., Gao, H., & Zhang, B. 2020, ApJ, 890, 102

Repeating Fast Radio Bursts from Pulsar-Asteroid Belt Collisions: Frequency Drifting and Polarization

Ze-Nan Liu
School of Astronomy and Space Science, Nanjing University
Nanjing 210023
Email: liuzenan@smail.nju.edu.cn

Fast radio bursts (FRBs) are a new kind of extragalactic radio transients. Some of them show repeating behaviors. Recent observations indicate that a few repeating FRBs (e.g., FRB 121102) present time–frequency downward drifting patterns and nearly 100% linear polarization. Following the model of Dai et al.(2016) who proposed that repeating FRBs may originate from a slowly-rotating, old-aged pulsar colliding with an asteroid belt around a stellar-mass object, we focus on the prediction of time–frequency drifting and polarization. In this scenario, the frequency drifting is mainly caused by the geometric structure of a pulsar magnetosphere, and the drifting rate–frequency index is found to be 25/17. On the other hand, by considering the typical differential mass distribution of incident asteroids, we find that an asteroid with mass $m \gtrsim 10^{17}$ g colliding with the pulsar would contribute abundant gravitational energy, which powers an FRB. A broad frequency band of the FRBs would be expected, due to the mass difference of the incident asteroids. In addition, we simulate the linear polarization distribution for the repeating FRBs, and constrain the linear polarization with $\gtrsim 30\%$ for the FRBs with flux of an order of magnitude lower than the maximum flux.

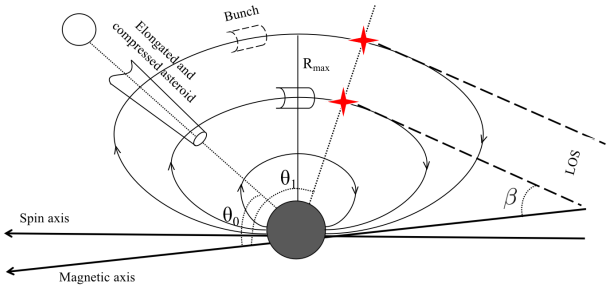

Figure 1: Schematic geometry of collision between an elongated, compressed asteroid and a pulsar, producing sub-burst downward frequency drifting of repeating FRBs. As the asteroid gradually falls with the immediate emergence of numerous net charges, a stray electric field outside of the asteroid has a component parallel to the magnetic field, which causes abundant bunches to leave from the surface of the asteroid and move along the magnetic field lines. A higher-frequency signal is generated closer to the pulsar due to a smaller curvature radius. The dashed lines display the line of sight (LOS) and θ_0 is the angle between the radial direction of the asteroid infalling and the magnetic axis. When the bunches move along the magnetic field lines sweeping across the LOS, the angle between the spark (marked by red stars) and the magnetic axis is represented by θ_1. β denotes the angle between the LOS and the magnetic axis.

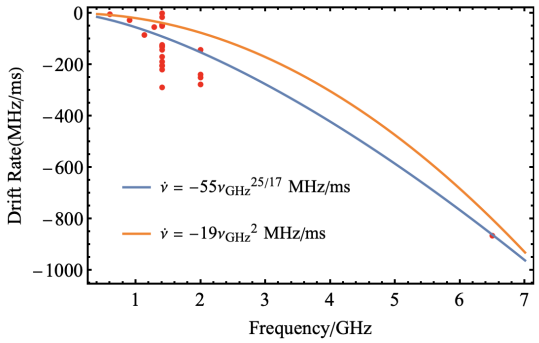

Figure 2: The drifting rate as a function of frequency. The red dots represent the observations of FRB121102. The blue line implied by Lorentz factor evolves with R, which shows a fitting curve to the observed data in our model. The orange line inferred by assuming that the Lorentz factor is a constant. We adopt the physical parameters: $\theta_0 = \pi/6$, $\theta_1 = \pi/3$, $\beta = \pi/2$.

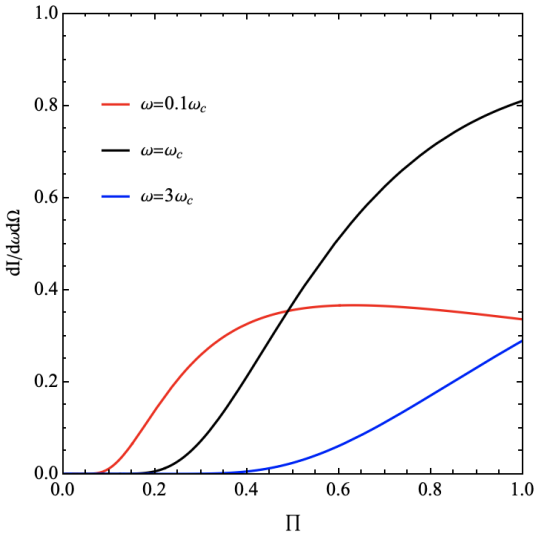

Figure 3: The curvature radiation of electrons as a function of the degree of the linear polarization. The unit of $dI/d\Omega d\omega$ is arbitrary and the parameter χ ranges from 0 to $10/\gamma$. The red, black and blue lines denote the angular frequency $\omega = 0.1\omega_c$, ω_c and $3\omega_c$, respectively, where ω_c is the characteristic frequency.

脉冲星B1937+21的奇特射电偏振角曲线可能由磁偶极场导致

卢吉光 (Jiguang Lu)
中国科学院国家天文台
北京 100101
Email: lujig@nao.cas.cn

脉冲星是高速旋转的强磁场致密星，辐射会由磁场两极处发出。 在早期研究脉冲星辐射机制的工作中，脉冲星磁场通常被假设为磁偶极场。 这样的假设导致了多种美妙的预言，比如S形偏振位置角曲线。 在强磁场中，发出辐射的带电粒子将沿着磁场线移动，而辐射会集中于粒子运动的方向，偏振方向为粒子运动曲线的主法线方向。 由于磁偶极场的磁场线都是平面曲线，所以辐射方向与偏振方向均与磁轴共面。 因此，当给定了一个磁倾角（磁轴与转轴的夹角）与视线角（转轴与视线方向的夹角）后，辐射相位与 偏振位置角之间存在一一对应关系。 这一模型称为旋转矢量模型，可以被用来拟合很多脉冲星的磁场几何，说明这些脉冲星的射电辐射几何由磁偶极场主导。

但是需要注意的是有些脉冲星的偏振位置角曲线很难用旋转矢量模型拟合，有时会认为这些偏振位置角曲线可能受到了多极场成分的影响。 通常认为脉冲星的强磁场是由中心致密星的磁矩产生的，显然这一磁矩不可能是纯偶极矩，而且多极场可以用来解释多种观测现象。 因此，多极场图像被广泛应用在脉冲星辐射模型中。 然而，尽管多种复杂观测现象能解使用多极场模型解释，不过模型会变得愈加复杂。 在多极场模型中，精确的脉冲星磁场位形难以计算，而脉冲星辐射几何也很难被构建得到。 我们应当承认脉冲星中一定存在多极场成分，但是这不应该是在我们遇到难以理解的新现象时用以推诿的借口。

脉冲星B1937+21是一颗毫秒脉冲星，它的偏振位置角曲线非常复杂，和旋转矢量模型预测的S形曲线截然不同。 然而，我们都知道一颗旋转脉冲星的磁场线会被转动扭曲，这会导致每一条磁场线都不再是平面曲线， 因此偏振位置角曲线会偏离旋转矢量模型的预测。 诚然，这种扭曲对于一般的辐射高度在10-1000公里左右的普通脉冲星来说是不显著的，但对于毫秒脉冲星却极其重要。 对于一颗周期2毫秒的脉冲星来说，它的磁层尺度大约只有100公里大，因此它的磁场在辐射区域是高度扭曲的。 这也自然地导致了一条偏离旋转矢量模型预测的偏振位置角曲线，这也为确定辐射几何的工作带来了极大的困难。

近期的FAST望远镜对脉冲星B1937+21进行的观测揭示了这颗星在脉冲峰之间的区域存在弱辐射， 这种弱辐射的偏振位置角看上去与旋转矢量模型的预测相似。 如果用旋转矢量模型对这一区域的偏振位置角进行曲线拟合，可以得到脉冲星的磁场位形参数。 通过这一偶极磁场的几何参数绘制出整个磁层中的磁场位形（如图1所示），可以对不同辐射相位中的偏振位置角进行预测，得到的结果与观测一致。 因此该脉冲星的偏振位置角曲线可能来自于转动扭曲后的磁偶极场。

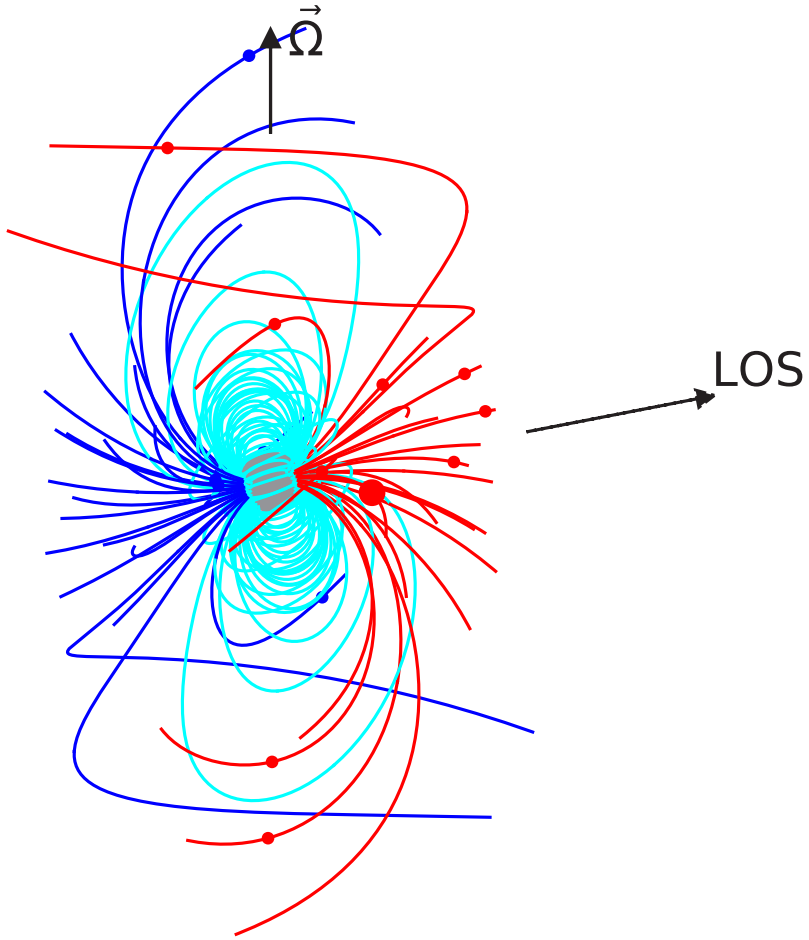

Figure 1: 依据实际比例绘制的脉冲星扭曲磁偶极场位形。红色线与蓝色线为分别自两极出发的开放磁场线，青色线为闭合磁场线，中心的灰色球为脉冲星。 磁场线上的红点与蓝点代表该处的辐射可以被望远镜接收到。

TransientX: A High Performance Transient Search Software

Yunpeng Men，*Vela*奖获得者
MAX PLANCK INSTITUTE for Radio Astronomy
Auf dem Huegel 69, D-53121 Bonn
Email: ypmen@mpifr-bonn.mpg.de

1 Introduction

Searches for fast radio transients have been widely investigated [1]. Transient search programs have also been developed on both CPU and GPU based algorithms, e.g. single_pulse_search.py of PRESTO and HEIMDALL. In this work, we will introduce a new high performance transient search software, TransientX, which is a cpu-based software but with comparable efficiency to GPU algorithms.

2 Algorithm

Data processing in TransientX can be divided into several successive tasks, including radio-frequency interference (RFI) mitigation, dedispersion, matched filtering, clustering and candidate plotting.

RFI mitigation
Better RFI mitigation can reduce the false-positive candidates, as well as improving the signal-to-noise ratio (S/N) of the true signals. TransientX provides several RFI remove algorithms, e.g. zapping the channels with known persistent RFI, zero-DM filter and zero-DM matched filter [2], which can be used in any combination to deal with various types of RFI.

Dedispersion
Correcting for the dispersion effect is important to improve the S/N of the signals. DM trials should be performed, because the DM is unknown in searches for unknown fast radio transients. Trivial dedispersion algorithms, based on aligning pulses in different frequency channels are very computationally expensive [3]. Therefore, several efficient algorithms have been proposed, e.g. subband dedispersion [4].

Matched filtering

Table 1: The simulation and search parameters.

Center frequency (MHz)	1250
Bandwidth (MHz)	500
Number of channels	4096
Time resolution (us)	50
Duration (s)	60
DM search range ($cm^{-3}pc$)	0-800
DM search step ($cm^{-3}pc$)	0.2
Width search range (ms)	0.05-100
Time elapse (s)	38

After dedispersion, TransientX performs the matched filtering for the pulse detection on DM trials, as in the BEAR algorithm [2]. The optimal detection statistics is

$$S/N = \frac{1}{\sqrt{N_{\rm box}}\sigma}\left(\sum_{|t-t0|\leq W} s(t)\right), \tag{1}$$

where $N_{\rm box}$ is the number of data points in the time span where $|t - t_0| \leq W$. In this step, a geometric series of pulse width will be searched. However, only the pulse width that maximizes the S/N is recorded, which is slightly different from BEAR [2].

Clustering
After dedispersion and matched filtering, we will get a S/N matrix of DM and pulse width. If there exists a bright pulse, we will see a group of points in the S/N matrix, with S/N larger than the threshold, because candidates with parameters deviating from the true value, which has limited smearing, can still have a large S/N. We would not like to record all of them, so we apply a clustering algorithm on the S/N matrix to remove the duplicate candidates. TransientX uses the Density-Based Spatial Clustering of Applications with Noise (DBSCAN) to perform the clustering, which has the advantage of high efficiency and independent from the shape of clusters.

Candidate Plotting
To make the candidate inspection user friendly, TransientX will produce a plot for each candidate, as shown in Fig. 1. The plot contains the meta information, profile, dynamic spectrum and the clustering view.

3 Benchmark

Even though TransientX is a cpu-based software, it has comparable efficiency to other GPU-based software, as is benefited by more efficient algorithms and better

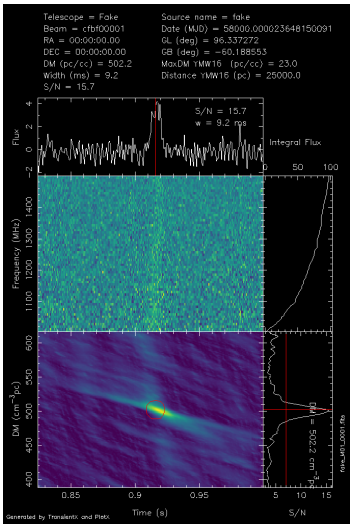

Figure 1: An example of the candidate plot.

optimization. We tested the TransientX using simulated data with the parameters shown in Table 1, and running TransientX on a single cpu core of Intel i7-10750H CPU. TransientX only needed about 38 s to finish the whole search pipeline, which means it is up to real-time transient search using CPU. TranisentX is a good pilot experiment for the transient search of future telescopes, such as the Square Kilometre Array (SKA).

References

[1] J. M. Cordes and M. A. McLaughlin. Searches for Fast Radio Transients. *ApJ*, 596(2):1142–1154, October 2003.

[2] Y. P. Men, R. Luo, M. Z. Chen, L. F. Hao, K. J. Lee, J. Li, Z. X. Li, Z. Y. Liu, X. Pei, Z. G. Wen, J. J. Wu, Y. H. Xu, R. X. Xu, J. P. Yuan, and C. F. Zhang. Piggyback search for fast radio bursts using Nanshan 26 m and Kunming 40 m radio telescopes - I. Observing and data analysis systems, discovery of a mysterious peryton. *MNRAS*, 488(3):3957–3971, September 2019.

[3] B. R. Barsdell, M. Bailes, D. G. Barnes, and C. J. Fluke. Accelerating incoherent dedispersion. *MNRAS*, 422(1):379–392, May 2012.

[4] A. Magro, A. Karastergiou, S. Salvini, B. Mort, F. Dulwich, and K. Zarb Adami. Real-time, fast radio transient searches with GPU de-dispersion. *MNRAS*, 417(4):2642–2650, November 2011.

从最初的意外发现到FAST脉冲星彩票的头奖－－球状星团脉冲星巡天中的惊喜不断

潘之辰 *(Zhichen Pan)*， 钱磊 *(Lei Qian)*
中国科学院国家天文台
*FAST*运行和发展中心
北京 *100101*
Email: panzc@bao.ac.cn, lqian@bao.ac.cn

这些故事的参与者和经历者包含了国家天文台、上海天文台、国家授时中心的诸多老师和同事，人数众多； 重要成员和相关合作已提及，如有遗漏请包含、指出！ 这里面的经验和教训，希望对于大家理解脉冲星搜索有用！

1 从FAST之前到FAST的脉冲星发现再到FAST的球状星团脉冲星发现

在获得FAST数据之前的脉冲星搜索准备中，我们已经幸运地在处理球状星团杜鹃座47中意外地找到了两颗新脉冲星，杜鹃座47 aa和ab（Pan et al. 2016）。 当时的我们，对于搜索发现后的timing一无所知，ab的timing在同一篇文章中由外国合作者完成，而aa的timing也由同样的外国合作者另发文章（Freire et al. 2018）。 时至今日，从中我的得到的深刻的经验和教训是，只搜索不timing相当于将重要的成果让于他人。

FAST的第一颗脉冲星发现于2017年8月4日的观测数据中，并且在同年8月6日的数据中得到验证。 其周期118.7 ms，色散33.9 pc cm^{-3}，位于纬度大约48度的北天。 而FAST第一颗认证的脉冲星（Qian et al. 2019）则是我们在Parkes多波束巡天的历史数据中找到了相同的信号而得以验证。 数十颗来自于漂移扫描的脉冲星发现，以及FAST跟踪的实现，使得我们在十月初计划通宵观测多个目标。 在这次观测中，我们发现了金牛座分子云中周期444 ms的Fermi脉冲星的射电信号（色散47.6 pc cm^{-3}），以及在球状星团中的脉冲星M92A（Pan et al. 2020）。 这是球状星团M92中的第一颗脉冲星！ 由于数据处理经验的缺乏和对于后续观测的无知，在发现后我们没有安排足够的后续的观测、没有及时向外界公布消息、也没有开展其监测和timing。 而更早之前，在2017年8月份的观测数据中我们即找到了FAST发现的第一颗毫秒脉冲星，临时名称为C8。 对于毫秒脉冲星特殊性的认识不足，使得我们将这些发现视同普通的发现而在第一时间错失了各种的机会。 从现在的观测结果来看，在FAST安装超宽带接收机的阶段，我们并没有安排长时间的对于球状星团的跟踪观测。 否则，我们将积累到非常重要的FAST低频球状星团观测数据，会将在2020年年底的一些脉冲星发现提前到2017年。

随着FAST跟踪范围的天顶角逐步扩大，我们终于得以观测更多的目标， 并顺利地在M14的3分钟数据找到了一颗色散82.1 pc cm^{-3}，周期1.98 ms的脉冲星。 当

时的无知使得我们忽视了在之前从未发现脉冲星的球状星团中发现脉冲星这一重要事件，错误地以为球状星团中能探测到1颗脉冲星是常态。 M14A目前已经获得了相位相连的timing结果，其轨道周期0.23天，伴星质量为1.8%太阳质量，是个典型的black widow。 从M92A的发现（20171019）到M14A的发现（20181219），间隔了正好整整14个月！

从FAST漂移扫描的实现到FAST跟踪的实现、从超宽带接收机到19波束L波段接收机，凝结了FAST大量的工作人员的心血。 这些利用调试期完成的发现，应证了他们已将望远镜调整到了最佳状态，使得我们可以尽早尽快地实现脉冲星发现。

FAST在2019年开展了风险共担科学观测的申请，我们，以及上海天文台的闫振老师，授时中心的罗近涛老师，一起都获得了观测时间用来完成球状星团脉冲星搜索和监测工作。 在搜索的最后我们迎来了来自于NGC6517和NGC6712的发现。NGC6517E是2019年6月28日发现的，由于数据处理的延迟，NGC6517F和G在2019年7月1日发现。 而在2019年6月28日夜，在检查NGC6712的4分钟观测数据中也发现了一颗新脉冲星NGC6712A。 这段时间正是在西安临潼国家授时中心举办FPS8会议。 这是在FPS会议期间发现的球状星团脉冲星！ 由于发现的时候缺少另一次观测数据的验证，我们并没有在FPS会议上临时宣布这些消息。 作为弥补，在FPS9会议上，我代表我们合作者向大家报告了这些发现以及完成的timing工作。 在2020年厦门的FPS9会议中，我们又有脉冲星发现。 我们在FAST指向LS-I +61303的观测数据中搜索到了色散大约241 pc cm^{-3}的一个信号。

我们已经连续两次在FPS会议期间实现了脉冲星的发现，希望在今后的FPS会议能一直举办，会议期间奇迹一直继续！

2 真正的头奖

从2019年7月开始，经历了超过十五个半月的脉冲星荒，我们没能在此期间找到任何一个球状星团脉冲星。 2020年10月初，因为工作需要，前往了FAST现场继续尝试基带数据处理；在处理的闲暇时间，考虑到服务器闲置，因此百无聊赖中找出了2019年FAST观测的球状星团数据开始了漫长的数据处理。 当时挑选的观测数据是2019年12月观测的M71和M53数据。选择这两个目标也不是完全的随机选择。 数据处理是串行进行的，分别在两个节点上处理M71和M53的数据。 令人意外地，在M71的数据处理结果中，一个周期79.9 ms的信号被发现。随后又找出了一个自转周期超过28 ms的信号。 这两个信号都具有宽带信号的特征，在另一次观测中都出现了。 当天半夜，我给所有相关和合作者发了消息，告知了M71B和M71C的发现。 这是自2019年7月后，15个多月后又迎来的脉冲星发现。 在贵阳看到了两个新脉冲星，M71B和C后，我就出发去了西安，到国家授时中心罗近涛老师处。 到的当晚，检查了M53的数据处理结果。 在排除了已知脉冲星信号后，又发现了三颗新脉冲星。 M53B相对较强，M53C很弱，但是证实都是新信号。 通过手工筛选，我们又看到了一个周期6.069 ms的微弱信号，即是脉冲星M53D的信号。

在西安的最后几天，我想到此前Duncan告诉我的，要尽量处理长的观测数据，以及Scott说的，你怎么能确定你找到的脉冲星就是这个球状星团里唯一的。 因此，我重新开始了M14和NGC6517的观测数据。 10月30日上午，我们在M14的观测数据中又找出了三个信号，虽然都很弱，但是信号特征清晰可见。 通过调整脉冲

星搜索结果的筛选（具体见Pan et al. 2020），2020年11月20日，我们又从M71的观测数据中找到了一个新的信号，M71D。 同样的方法让我们在2020年11月24日从NGC6517数据中又找到了两个更加暗弱的信号， 以及在2020年11月27日找到了M14E。 M14E是个很有有意思的redback，轨道周期0.85天，具有掩食现象，我们已经实现了它的timing。

我们以为已经实现了球状星团脉冲星10%的数量增加，没想到精彩还在后头。2020年12月1日， 在搜索结果中看到了一个2.65 ms的信号。 这个信号的周期和已知的M5B的三次谐波非常接近，最先被认为就是谐波。 随后的的timing证实其实轨道周期1.6天伴星质量0.2倍太阳质量的双星，是一个新的脉冲星M5F。 类似的，我们找到了M3E。 它的周期是5.47 ms，和M3D的5.44 ms非常接近。 直到我们检查了历史观测数据，同时看到了5.44 ms和5.47 ms的信号，才相信这是个新的脉冲星。 M3E是双星，轨道周期7.1天，伴星0.2倍太阳质量。

2020年12月16日，是发现的顶峰。检查之前运行的M10的数据处理中，一下子找到了两个信号，M10A和B。 这是M10中首先发现的两个脉冲星。 随后是M15I的发现。 2020年9月22日的M15观测，中间中断了大约8000秒。 中断的8000秒，我们发现脉冲星信号也相应中断了，而干扰信号却持续。 根据这一规律，我们发现了M15I，而且因为这个间断相当于是将以此观测分为两次，我们认为M15I在这天的观测中被发现和验证了。 当天下午，我们一下子找到了M2中的4个脉冲星，M2A、B、C和D。 我们又将数据处理了一遍，并在当日深夜（其实已经17日了）找到了M2E。 M2E的发现并没有使用任何筛选和排序程序，是我用肉眼看原始搜索结果看出来的。 这一天我们一共找到了8个脉冲星！ 2020年12月19日，也是通过肉眼看原始观测数据的方法，找到了脉冲星M3F。 M3F目前轨道已经确定，是轨道周期1.6天的双星，伴星也是小质量恒星。 2021年2月20日，我们找到了M12A，这是M12中的首个脉冲星发现。

通过使用FAST发现的球状星团脉冲星，除了这里提到的30个以外，还有已经发表成文的M13F（Wang et al. 2020）以及2020年年底发现的M5G，共32个； 另有M3A和M13E（Wang et al. 2020）是由FAST验证了轨道。 这32颗脉冲星现在就像中奖之后的又32张彩票。 它们的各种性质或许还会在今后很长的一段时间内给我们带来更多的惊喜。 目前，这些工作已经涉及了5篇文章（M92A，Pan et al. 2020; M13E和F，Wang et al. 2020；NGC6517E/F/G，Pan et al. accepted by RAA；NGC6712A，Yan et al. submitted to ApJ；24颗脉冲星发现，Pan et al. submitted to ApJL）， 我们也申请了相关的国家自然科学基金和2021年的FAST观测时间。目前人类在36个球状星团中找到了225个脉冲星。 虽然FAST受限于观测天区，我们只能观测到160球状星团中的45个。 我们实现了球状星团脉冲星总数15%的发现增量， 以及在FAST天区中我们将球状星团脉冲星数目实现了翻倍！可以想象，如果今后的望远镜阵能实现更大天区覆盖，这样的惊喜还会源源不断的产生，其中或许会为我们带来脉冲星-中子星系统、双脉冲星系统、毫秒脉冲星-毫秒脉冲星系统、甚至是脉冲星-黑洞这样的新发现。

最后，祝愿能保持已经延续了两年的幸运，即在今年的FPS会议期间依然有脉冲星发现！

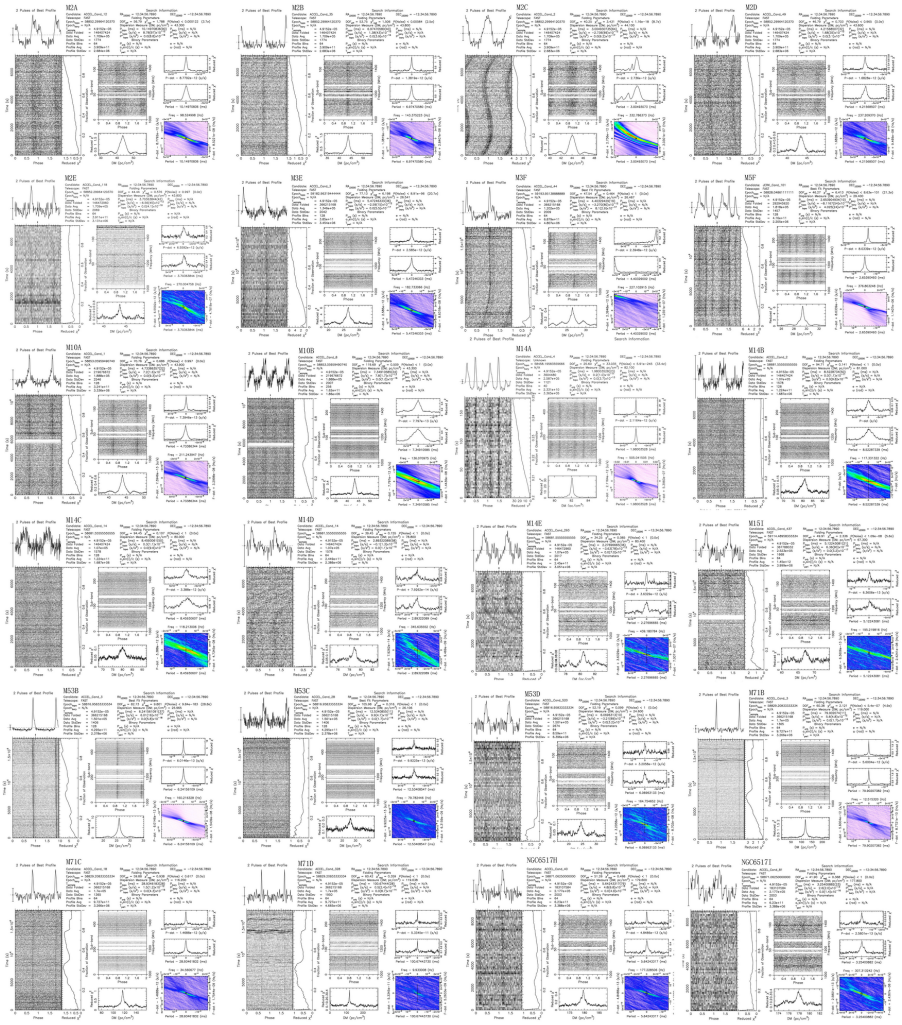

Figure 1: 在2020年10月起的两个月时间内发现的24颗脉冲星。

3 参考文献

Dai S., Johnston S., Kerr M., et al., 2020, ApJ, 888, 18

Freire P. C. C., Rildolfi A., 2018, MNRAS, 476, 4794

Pan Z., Hobbs G., Li D., et al., 2016, MNRASL, 459, 26

Pan Z., Ma X., Qian L., et al., RAA in press

Pan Z., Ransom S. M., Lorimer D. R., et al., 2020, ApJL, 892, 6

Qian L, Pan Z., Li D., et al., 2019, SCPMA, 6259508Q

Wang L., Peng B., Stappers B. W., et al., 2020, ApJ, 892, 43

Yan Z., Pan Z., et al., submitted to ApJ

FAST球心ITRF坐标

钱磊 *(Lei Qian)*
岳友岭 *(Youling Yue)*
中国科学院国家天文台
北京 *100101*
Email: lqian@nao.cas.cn; ylyue@nao.cas.cn

脉冲星搜索及测时软件都需要提供台站某个不动点的ITRF坐标（X, Y, Z）。对于FAST而言，不动点可以取为球心。在使用各种软件的过程中，我们发现不同人使用的台站坐标有所不同。在此，我们试图正本清源。

大地测量得到，在WGS-84坐标系中，FAST球心的经度纬度和大地高分别为$\lambda = 106°51'24.000740"$、$\phi = 25°39'10.626537"$ 和$h = 1110.028801$ m。ITRF和WGS-84所用的椭球几乎相同，相差在1米之内，所以直接采用WGS-84椭球进行计算。经纬度转换为(X, Y, Z)的公式为

$$\begin{aligned} X &= (N+h)\cos\phi\cos\lambda \\ Y &= (N+h)\cos\phi\sin\lambda \\ Z &= [N(1-e^2)+h]\sin\phi \end{aligned}$$

其中$N = a/\sqrt{1-e^2\sin^2\phi}$，而长轴$a = 6378137$ m，短轴$b = 6356752.3142451795$ m，偏心率$e^2 = \frac{a^2-b^2}{a^2}$。

由此计算得到$(X, Y, Z) = (-1668557.2070983793, 5506838.5266271923, 2744934.9655897617)$。岳友岭计算并提供给PINT的值为$(X, Y, Z = (-1668557.0, 5506838.0, 2744934.0))$，相差在1.2米以内。根据和岳有岭的讨论，他在计算时向下取整，所以我们认为这两个结果是一致的。我们认为PINT 目前使用的FAST 坐标是可用的，但我们的结果更为准确。而更准确的坐标需要长期的脉冲星计时以及VLBI 观测确定。

FAST/Future Pulsar Symposium 9 (FPS9)
Aug. 28-30, 2020, Xiamen University, Xiamen - P. R. China
http://psr.pku.edu.cn/fps/FPS9/FPS9.html

Estimating the maximum gravitational mass of non-rotating neutron stars from the GW170817/GRB 170817A/AT2017gfo observations

邵东生 *(Dong-Sheng Shao)*
中国科学院紫金山天文台
南京 *210033*
Email: shaods@pmo.ac.cn

Abstract

Assuming that the differential rotation of the massive neutron star (NS) formed in the double NS (DNS) mergers has been effectively terminated by the magnetic braking and a uniform rotation has been subsequently established (i.e., a supramassive NS is formed), we analytically derive in this work an approximated expression for the critical total gravitational mass ($M_{\rm tot,c}$) to form supramassive NS (SMNS) in the DNS mergers, benefited from some equation of state (EoS) insensitive relationships. The maximum gravitational mass of the non-rotating NSs ($M_{\rm TOV}$) as well as the dimensionless angular momentum of the remnant (j) play the dominant roles in modifying $M_{\rm tot,c}$, while the radius and mass differences of the pre-merger NSs do not. The GW170817/GRB 170817A/AT2017gfo observations have provided so far the best opportunity to quantitatively evaluate $M_{\rm TOV}$. Supposing the central engine for GRB 170817A is a black hole quickly formed in the collapse of an SMNS, we find $M_{\rm TOV} = 2.13^{+0.09}_{-0.08} M_\odot$ (68.3% credibility interval, including also the uncertainties of the EoS insensitive relationships), which is consistent with the constraints set by current NS mass measurements.

1 The critical total gravitational mass for forming SMNS in DNS merger

In the scenario of DNS merger,we found the critical total gravitational mass for forming SMNS in DNS merger satisfies,

$$\begin{aligned} M_{\rm tot,c} \approx & 0.924 M_{\rm TOV}(1 + 7.94\times10^{-2}\zeta_{\rm TOV}^{-1} j^2 + 1.70\times10^{-2}\zeta_{\rm TOV}^{-2} j^4) \\ & \times (0.8634 + 1.051\zeta_{\rm TOV})(1 - 0.091\ M_\odot^{-1}\ m_{\rm loss}) + m_{\rm loss} \end{aligned} \quad (1)$$

where $j \equiv cJ/GM^2$ is the dimensionless angular momentum, $\zeta_{\rm TOV} = GM_{\rm TOV}/R_{\rm TOV}c^2$ is the compactness of the neutron star in the maximum configuration of non-rotating state, and $m_{\rm loss}$ is all the mass outside of the remnant core, including the masses of surrounding torus and the ejecta.

2 The estimate of $M_{\rm TOV}$ with GW170817

In the case of GW170817, assuming the central engine for GRB 170817A/AT2017gfo was a black hole quickly formed in the collapse of a SMNS at $t_{\rm coll} \sim 1$ s, we implemented Monte Carlo sampling to obtain the probability density distributions of $j_{\rm coll}$(the dimensionless angular momentum at the onset of collapse) and $M_{\rm TOV}$(see Fig.1).Our result of $M_{\rm TOV} = 2.13^{+0.09}_{-0.08} M_\odot$ is consistent with current bounds set by the NS mass measurements as well as some theoretical investigations (see Fig.2).

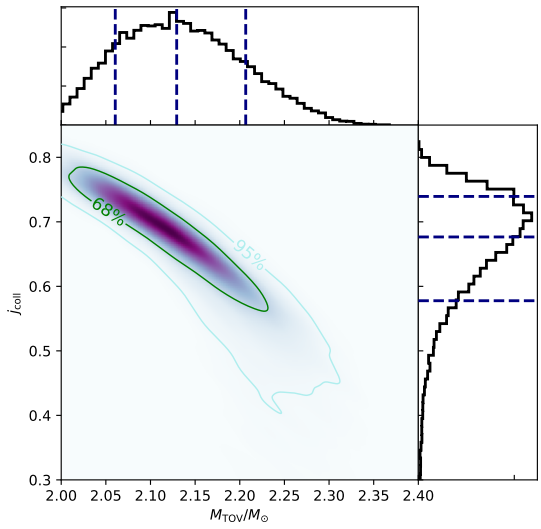

Figure 1: The probability density of $j_{\rm coll}$ and $M_{\rm TOV}$ in the case of GW170817/GRB 170817A/AT2017gfo.

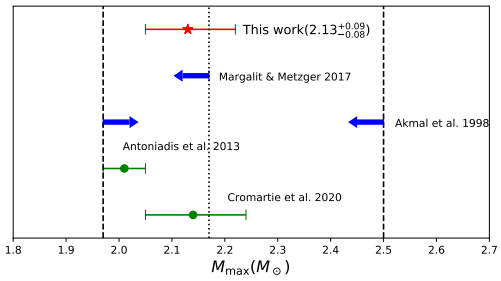

Figure 2: Constraints and records of $M_{\rm TOV}$. The dash black lines are the lower and upper limits on $M_{\rm TOV}$, respectively.

用脉冲星计时“称”引力子的质量

邵立晶 *(Lijing Shao)*
北京大学科维理天文与天体物理研究所
北京 *100871*
Email: lshao@pku.edu.cn

脉冲星是天空中精准的“钟表”。脉冲星计时（Pulsar Timing）通过用简单的、相对论性的理论模型—即，脉冲星计时模型（Pulsar Timing Model）—联结脉冲星与地球上的原子钟的固有时，通过对脉冲星计时数据的拟合，可以测量诸多有趣的物理内容。

在本次会议上，我简单介绍了我们组用脉冲星计时“称”引力子质量的工作，主要发表在

- Miao, X., Shao, L., & Ma, B.-Q. 2019, *Bounding the mass of graviton in a dynamic regime with binary pulsars*, Phys. Rev. D 99, 123015
- Shao, L., Wex, N., & Zhou, S.-Y. 2020, *New graviton mass bound from binary pulsars*, Phys. Rev. D 102, 024069

在爱因斯坦的广义相对论里，引力子是质量**严格**为零的粒子。倘若引力子的质量非常小、但不为零，这在基本物理学中将是完全不等价于广义相对论的情形，会对基本物理学产生**冲击性**的影响。所以，从实验的角度去测量引力子的质量变得非常重要。脉冲星计时，为我们提供了一个绝好的工具！它带给我们完全不同于太阳系中用 Yukawa 静态势能、引力波中用修正的运动学意义的色散关系的实验检验。

欢迎有兴趣的同仁阅读、指正我们的工作。

磁星扭曲磁场和开放磁力线区物理

仝号 *(Renxin Xu)*
广州大学物理与材料科学学院
广州 *510006*
Email: htong_2005@163.com

磁星(magnetar)一般认为是年轻的强磁场的中子星. 它们的磁场可以高达10^{14}-10^{15} G, 是通常脉冲星磁场的约100倍, 高于量子电动力学的临界磁场4.4×10^{13} G. 强磁场意味着更多的磁能储备, 从而有可能解释磁星的持续的X-射线辐射, 和各种爆发活动. 这就是磁星模型大的框架.

人们认为, 通常脉冲星就是中子星加偶极磁场, 磁星是中子星加扭曲的偶极磁场(Thompson et al. 2002, ApJ, 574, 332). 这有可能解释为什么有些中子星表现为通常脉冲星, 有些中子星表现为磁星. 这就是磁星扭曲的磁场. 对这个图像的建模, 前人一般认为磁星的自转周期约为10秒, 因此极冠区很小, 从而忽略磁星磁层的开放磁力线区, 只考虑闭合磁力线区. 这么做的一个后果就是, 通常脉冲星的磁层物理都是在开放磁力线区, 磁星磁层的物理都是在闭合磁力线区. 脉冲星和磁星磁层无法实现自然的统一.

我们指出(Tong 2019, MNRAS, 489, 3769), 前人以为磁星极冠区很小, 是基于偶极磁场, 但是磁星的磁场不是偶极场. 自洽的计算应该是针对一个扭曲的偶极磁场, 计算它的极冠区和开放磁力线区物理. 我们的计算表明, 在扭曲磁场下, 磁星的极冠区可以达到1-2公里, 有可能对应磁星观测上的热斑大小. 磁星开放磁力线区的粒子外流将导致磁星扭曲磁场的解扭. 从而有可能解释磁星爆发时的X-射线光度随时间的演化. 考虑磁星开放磁力线区物理, 可以自然的得到磁星和通常脉冲星的统一. 磁星磁层开放磁力线区有着丰富的物理.

Pulsar glitch in a strangeon star model

汪卫华 *(Weihua Wang)*
北京大学物理学院
北京 *100871*
Email: wang-wh@pku.edu.cn

Glitch is supposed to be a probe into pulsar's interior. Currently, the most acceptable scenario for glitch is the superfluid vortex model, but the starquake model remains possible. The absence of radiative and pulse profile changes, moreover, the hundreds of days of post glitch relaxation time, are supposed to be signatures of internal origin of the glitch. The superfluid vortex model, which interprets glitch as the abrupt angular momentum from the faster-rotating crustal superfluid component to the crust (and that coupled to it), becomes popular due to its great success in describing the post glitch recovery process [1, 2]. Efforts have made to give constraints on neutron star (NS) properties through glitch statistics, among which the glitch activity parameter [3], which reflects the lower limit of the fractional moment of inertia of the superfluid component that weakly coupled to the crust, is of particular importance.

However, most recent observations show clearly that, glitch can induce radiative and/or pulse profile changes in normal radio pulsars, high magnetic field pulsars and magnetars in X-ray and/or radio bands [4, 5, 6, 7]. These new observational evidences probably indicate an unified physical origin of glitch. Therefore, it is meaningful to explore to what extent the glitch activity parameter can be reproduced in the solid strangeon star model in the framework of starquake secnario.

We present parameters needed to define the glitch activity first. The total energy of the solid star is

$$E_{\rm total} = E_0 + \frac{L^2}{2I} + A\varepsilon^2 + B(\varepsilon - \varepsilon_0)^2, \tag{1}$$

where E_0 is the total energy of a non-rotating star, $L^2/2I$ is the rotating energy, L is the total angular momentum, I is the total moment of inertia (reduces to I_0 neglecting rotation), $A\varepsilon^2$ is modification of gravitational energy of an ellipsoid relative to a spheroid star with the same mass and density, $A = (3GM^2)/(25R)$, the fourth term in Eq.(1) is the elastic energy, $B = \mu V/2$, μ is the shear modulus and $V = 4\pi R^3/3$ is the star's volume, ε_0 is the reference oblateness, R is the radius of the star. Glitch activity is defined as

$$\dot{\nu}_{\rm g} = \frac{\sum_i \sum_j \Delta\nu_{ij}}{\sum_i T_i}, \tag{2}$$

where $\Delta\nu_{ij}$ represents change in frequency due to glitch j in pulsar i, and T_i is the total observation time over which pulsar i has been searched for glitches. In the

starquake scenario, the total moment of inertia can be given by

$$I = I_0(1+\varepsilon)(1+\eta), \Delta I \simeq -I_0\Delta\varepsilon - I_0\Delta\eta, \tag{3}$$

where ε is the oblateness of the star, η describes the degree of density uniformity, $\Delta\varepsilon$ and $\Delta\eta$ are changes in oblateness and density uniformity. Glitch size is equal to the decrease in the total moment of inertia of the star,

$$\frac{\Delta\nu}{\nu} = -\frac{\Delta I}{I} = \Delta\varepsilon_{\rm m} + \Delta\eta, \Delta\varepsilon_{\rm m} = k\Delta\varepsilon, \tag{4}$$

where k describes the over recovery during glitch. $\Delta\varepsilon$ and $\Delta\eta$ are connected through the recovery coefficient Q,

$$Q = \frac{\Delta\varepsilon_{\rm m} - \Delta\varepsilon}{\Delta\varepsilon_{\rm m} + \Delta\eta} = \frac{(k-1)\Delta\varepsilon}{k\Delta\varepsilon + \Delta\eta}. \tag{5}$$

Finally, we arrive at the glitch activity in strangeon star,

$$\dot{\nu}_{\rm g} = (\frac{k-1}{Q}\frac{B}{A(A+B)}2\pi^2\nu^2 I_0)|\dot{\nu}|, \tag{6}$$

where $\dot{\nu}$ is the spin down rate. Comparison between Eq.(6) and $\dot{\nu}_{\rm g} = 0.01|\dot{\nu}|$ presented by Fuentes et al. indicates that, parameters A and B should fulfill the relation

$$A \simeq B, \mu \simeq 3\times10^{34}(\frac{M}{1.4\ M_\odot})^2(\frac{R}{10\ {\rm km}})^{-4}\ {\rm erg/cm^3}, \tag{7}$$

where $M_\odot$ is the mass of the Sun.

We conclude that, the shear modulus of the solid strangeon star should be about several times 10^{34} erg/cm^3 in order to explain the statistical glitch activity relation.

References

[1] Anderson P. W., Itoh N., 1975, Nature, 256, 25

[2] Alpar M. A., Anderson P. W., Pines D., Shaham J., 1984, ApJ, 276, 325

[3] Fuentes J. R., Espinoza C. M., Reisenegger A., Shaw B., Stappers B. W., Lyne A. G., 2017, A&A, 608, A131

[4] Akbal O., Gügercinoğlu E., Şaşmaz Muş S., Alpar M. A., 2015, MNRAS, 449, 933

[5] Kaspi V. M., Beloborodov A. M., 2017, Ann. Rev. Astro. Astrophys., 55, 261

[6] Palfreyman J., Dickey J. M., Hotan A., Ellingsen S., van Straten W., 2018, Nature, 556, 219

[7] Feng H., Li H., Long X. Y., Bellazzini R., et al. 2020, Nature Astronomy, 4, 511, doi:10.1038/s41550-020-1088-1

On the Magnetospheric Origin of Repeating Fast Radio Bursts

Weiyang Wang
National Astronomical Observatories, Chinese Academy of Sciences
Beijing 100101
Email: wywang@bao.ac.cn

A bright radio burst was newly discovered in SGR 1935+2154, which exhibits some fast radio burst (FRB)-like temporal and frequency properties, suggesting a neutron star (NS)/magnetar magnetospheric origin of FRBs. We propose an explanation of the temporal and frequency properties of sub-pulses of repeating FRBs based on the generic geometry within the framework of charged-bunching coherent curvature radiation in the magnetosphere. The sub-pulses in a radio burst come from bunches of charged particles moving along different magnetic field lines. Their radiation beams sweep across the line of sight at different times, and those radiating at the more curved part tend to be seen earlier and at higher frequency. However, by considering bunches generated at slightly different times, we find there is also a small probability that the emission from the less curved part can be seen earlier. The observed interval is given by

$$\Delta t_{\rm obs} = \Delta t_{\rm geo} + t_{20} - t_{10}, \tag{1}$$

where $\Delta t_{\rm geo}$ is the geometric time delay, which can be written as

$$\Delta t_{\rm geo} = \frac{s_2 - s_1}{v_e} - \frac{\Delta r \cos\theta_p}{c}, \tag{2}$$

where $\Delta r \cos\theta_p$ is the projection of the distance between the two emitting points in the direction of the LOS. We simulate the time–frequency structures by deriving various forms of the electric acceleration field in the magnetosphere. Our model model predicts that most FRBs would have downward-drifting subpulses, but there are also upward-drifting events, and one would be more likely to observe these from FRBs with long duration. This structure of sub-pulses is a natural consequence of coherent curvature radiation from an NS/magnetar magnetosphere with suddenly and violently triggered sparks. We apply this model to explain the time–frequency structure within a specific dipolar configuration by invoking the transient pulsar-like sparking from the inner gap of a slowly rotating NS, and we have also applied it to more generic configurations.

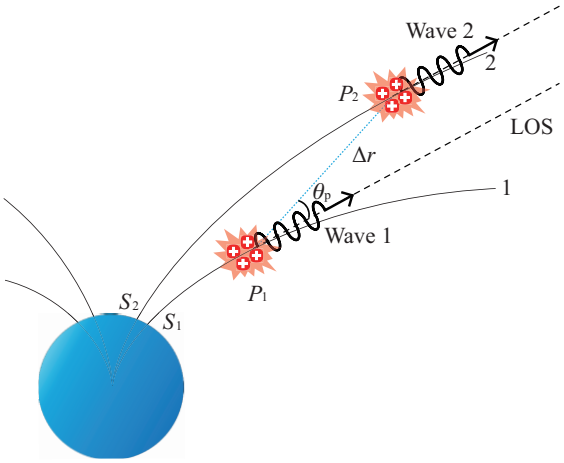

Figure 1: Schematic diagram of the neutron star/magnetar magnetosphere and radiation particle bunches. For instance, two magnetic field lines with charged bunches stream outflow are plotted. The dashed lines show the LOS. P_1 and P_2 denote the points where emissions can sweep the LOS at two magnetic field lines, i.e. two emitting points. Here, we assume that the curvature radius at P_1 is smaller than that at P_2. S_1 and S_2 denote the locations where the two bunches generation.

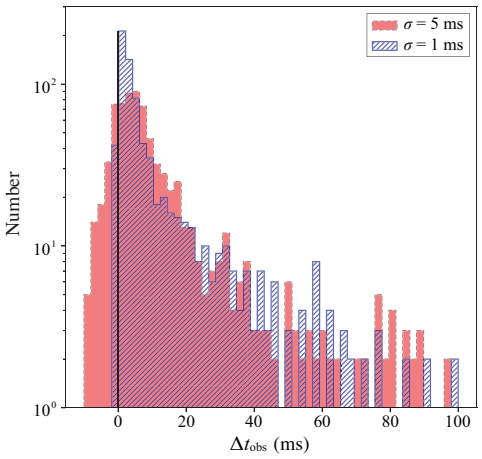

Figure 2: Histograms of estimated $\Delta t_{\rm obs}$. The time delay due to the un-simultaneous sparking is assumed as normally distribution with $\mu = 0$ and $\sigma = 1\,$ms, (blue) 5 ms (red). The $\Delta t_{\rm geo}$ is simulated by making the $\sin\theta_s$ uniformly distributed when θ_s varies in $0 - 0.02$. The vertical black solid line divides events with positive/negative values. We found in most cases that the emissions from the more-curved parts of the field lines are seen earlier than those from the less-curved parts.

“三味”三角形

徐仁新 (Renxin Xu)
北京大学物理学院
北京 100871
Email: r.x.xu@pku.edu.cn

对称性在粒子物理学上的重要性以杨振宁之语[1]“*Symmetry dictates interaction*”为标志，振聋发聩、响彻科坛（如David Gross一文[2]）。脉冲星肚子里到底“卖”什么货？ 这里提醒：澄清该极致密物态之谜亦不能忽略对称性扮演角色。

下面要谈的这种对称性不是几何的，而是跟夸克的味道有关。 粒子物理标准模型认为共存在六味夸克：$\{u, d, s; c, t, b\}$（称前三者为轻味夸克，质量 $<\sim 0.1$ GeV；后三者为重味夸克，质量 $>$ GeV），诚然人们还不明白为何会有“六味”。如果某个系统内几味夸克的数目基本上差不多，就称作“味对称”的（可能存在少许对称性破缺）；反之，若几味夸克的数目相差很明显即为“ 味不对称”的。

基本强相互作用的强度决定了零压情况下强物质的密度（价夸克间距$\Delta x \sim 0.5$fm），从而也给出典型的夸克动力学能量尺度$\hbar c/\Delta x \sim 0.5$GeV。 可见轻味夸克主导零压强物质。鉴于$u$、$d$质量太接近，可以相信应存在两味强物质，即原子核。

会有三味的强物质吗？这跟强物质的一个特点有关：大量电子会伴随两味物质而存在，但几乎不出现在三味物质中！ 三味物质显然不可能构成生命，但也有一大优势：大块三味强物质可因缺电子而比两味强物质更稳定。 Landau在不了解“三味”之时推测了两味极端不对称的“中子物质”星，但三味对称的强物质可能为自然所喜欢。如下三角形刻画了这一点，或在某种意义上体现了物理学中对称性精神。

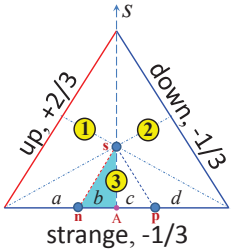

Figure 1: 三味三角形，其内任一点刻画三味夸克的数密度（$\{n_{\rm u}, n_{\rm d}, n_{\rm s}\}$分别代指上、下、奇异夸克，数值则由该点相对某边的高决定）。 点“s”位于三角形中心，线“sn”、“sp”分别平行于上、下夸克边，轴“S”衡量奇异数且其上任一点具有完美的同位旋对称性。 原子核位于“A”点附近，中子星和质子星分别位于“n”、“p”处。

[1]Yang, C.-N. *Einstein's impact on theoretical physics.* Physics Today, 1980, 33 (6) 42-49.
[2]Gross, D. J. *The role of symmetry in fundamental physics.* PNAS, 1996, 93, 14256 - 14259.

The first evidence for three-dimensional spin-velocity alignment in PSR J0538+2817

Jumei Yao，*Crab*奖获得者
National Astronomical Observatories, Chinese Academy of Sciences
Xinjiang Astronomical Observatories, Chinese Academy of Sciences
Beijing 100101
Email: yaojumei@xao.ac.cn

More than 50 years after the discovery of pulsars and confirmation of their association with supernova explosions, the origin of the initial spin and velocity of pulsars remains largely a mystery. The typical space velocities of several hundred km s^{-1} have been attributed to "kicks" resulting from asymmetries either in the supernova ejecta or in the neutrino emission. Observations have shown a strong tendency for alignment of the pulsar space velocity and spin axis in young pulsars but, up to now, these comparisons have been restricted to two dimensions. We report here the first evidence for three-dimensional alignment between the spin and velocity vectors, largely based on observations made with the Five-hundred-meter Aperture Spherical radio Telescope (FAST) toward the pulsar PSR J0538+2817 and its associated supernova remnant (SNR) S147. Analyses of the pulsar interstellar scintillation, the pulse polarization of PSR J0538+2817, and proper motion measurements were used to determine the location of the pulsar within the SNR and hence its radial velocity. Current supernova simulations have difficulty producing such 3D alignment. Our results, which depend on the unprecedented instantaneous sensitivity of FAST, add another dimension to the intriguing correlation between pulsar spin-axis and birth-kick directions, thus deepening the mysteries surrounding the birth of neutron stars.

Fig. 1 illustrates the 3D relationship of the derived pulsar velocity and spin vectors. On the plane of the sky, the position angle offset between the projected velocity and spin axis estimated from polarization PA fitting $\Delta\Psi_{\rm pm\_pol} = 4^\circ.5 \pm 1^\circ.7$ is consistent with $\Delta\Psi_{\rm pm\_X} = 3^\circ.0 \pm 5^\circ.8$, where the spin axis is derived from X-ray torus modelling, further comfirming 2D approximate alignment. The inclination angles are less well determined, especially ζ_v derived from ISS analysis. However, except for the incliantion angle of spin axis given by X-ray torus modelling, ζ_v and $\zeta_{\rm pol}$ obtained from FAST polarization and ISS analysis overlap well within the uncertainties: $\Delta\zeta_{\rm v\_pol} = 6^\circ \pm 14^\circ$. In the lower panel of Fig. 1, we show the 3D relationship of the vectors with the 1-σ and 2-σ uncertainties in their orientation.

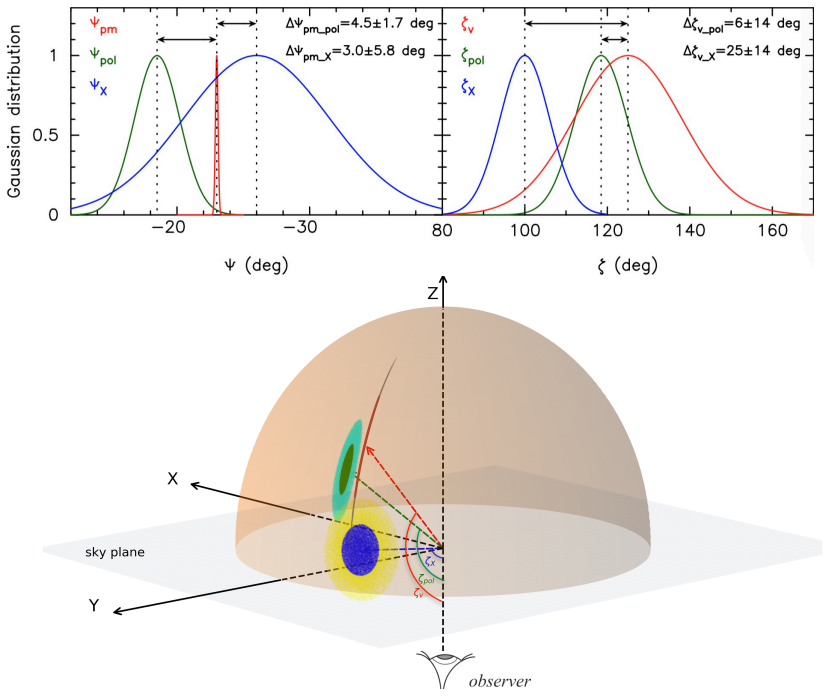

Figure 1: Position angles ψ and inclination angles ζ of the spin axis and velocity vector (upper panels) and the corresponding 3D distribution on the surface of a unit sphere (lower panel). In the upper panels, the spin-vector constraints estimated from polarization PA fitting and X-ray torus fitting are shown in dark green and blue respectively, and the velocity-vector constraints obtained from VLBI (position angle) and the ISS analysis (inclination angle) are shown in red. The lower panel shows the 1-σ and 2-σ 3D constraints for the vector orientations, in dark green and light green for the spin obtained from PA fitting and in blue and yellow for the spin given by X-ray torus fitting, and in red and gray for the velocity.

Pulsar Observation and Study with FAST and Parkes Radio Telescope

Lei Zhang，*Vela*奖获得者
School of Physics and Technology, Wuhan University, Wuhan 430072, China
Email: leizhang996@bao.ac.cn

Pulsars are dense objects. They emit beams of radiation that are often detected using radio telescopes. Not only are they rich in radiation phenomena, natural laboratories for studying the nature and physical laws of materials under extreme conditions, but also probes for studying interstellar media, gravitational waves and their generation processes. Pulsar search is the most important study for related topics such as pulsar astrophysics and applications. It is also one of the top scientific priorities of the Five-hundred-meter Aperture Spherical radio Telescope (FAST) in its early scientific stage. During my Ph.D. study, I participated in the FAST pulsar search, assisted FAST to complete the breakthrough of zero discovery of pulsars by using Chinese equipment, and relied on FAST and Parkes 64m radio telescope to study the pulsar radiation phenomenon in detail.

We describe PSR J1926−0652, a pulsar recently discovered with the FAST. Using sensitive single-pulse detections from FAST and long-term timing observations from the Parkes 64-m radio telescope, we probed phenomena on both long and short time scales. The FAST observations covered a wide frequency range from 270 to 800 MHz, enabling individual pulses to be studied in detail. The pulsar exhibits at least four profile components, short-term nulling lasting from 4 to 450 pulses, complex subpulse drifting behaviours and intermittency on scales of tens of minutes (see in Figure 1). While the average band spacing P_3 is relatively constant across different bursts and components, significant variations in the separation of adjacent bands are seen, especially near the beginning and end of a burst. Band shapes and slopes are quite variable, especially for the trailing components and for the shorter bursts. We show that for each burst the last detectable pulse prior to emission ceasing has different properties compared to other pulses. These complexities pose challenges for the classic carousel-type models More details see in Zhang et al., 2019, ApJ, 877:55.

We report the first wideband observations of pulsars C, D and J in the globular cluster 47 Tucanae (47 Tuc or NGC 104) using the Ultra-Wideband Low (UWL) receiver system recently installed on the Parkes 64 m radio telescope. The wide frequency range of the UWL receiver (704–4032 MHz), along with the well-calibrated system, allowed us to obtain flux density measurements and polarization pulse profiles. The mean pulse profiles have significant linear and circular polarization, allowing

for determination of the Faraday rotation measure for each pulsar. Precise measurements of the dispersion measures show a significant deviation in the value for pulsar D compared to earlier results. Searches for new pulsars in the cluster are on-going and we have determined optimal bands for such searches using the Parkes UWL receiver system. More details see in Zhang et al., 2019, ApJL, 885:L37.

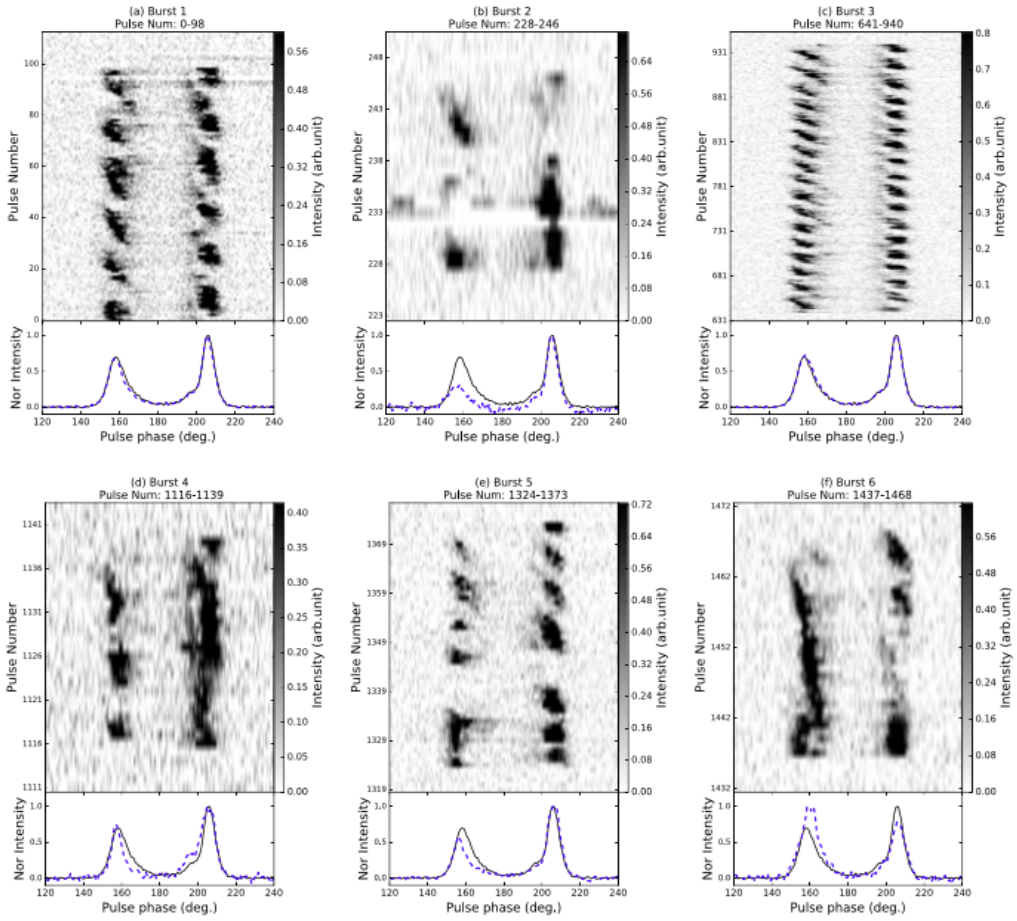

Figure 1: Pulse stacks for each burst are given in the upper panel of each subplot. The lower panel of each subplot shows the pulse profile averaged over the whole data span as a black solid line and averaged over the particular burst state as a blue dashed line.

来自脉冲星极冠区的软伽马射线辐射

朱羿元（*Yiyuan Zhu)*
华中科技大学 天文学系
武汉 *430074*
Email: zhuyiyuan1997@qq.com

脉冲星极冠区的级联过程是脉冲星最基础的物理过程之一，脉冲星周围的等离子体大气的产生和脉冲星风等都与该过程有关，然而在脉冲星高能辐射的观测中，并没有来自极冠区级联过程的直接观测证据。脉冲星的GeV辐射主要来自于光速圆柱附近的外磁层。脉冲星的非热X射线辐射来源仍然存在争议。而所谓的MeV脉冲星可能是辐射来自极冠区级联过程的重要证据。

为了探究这种可能性，我们模拟了脉冲星极冠区的级联过程，计算了脉冲星在不同周期、磁场强度和磁场线曲率半径下的粒子产率（图 1）和总光度（图2）,把模拟结果和MeV脉冲星的观测结果相比较3，我们认为MeV脉冲星的软伽马射线辐射是来自于脉冲星极冠区的级联过程。

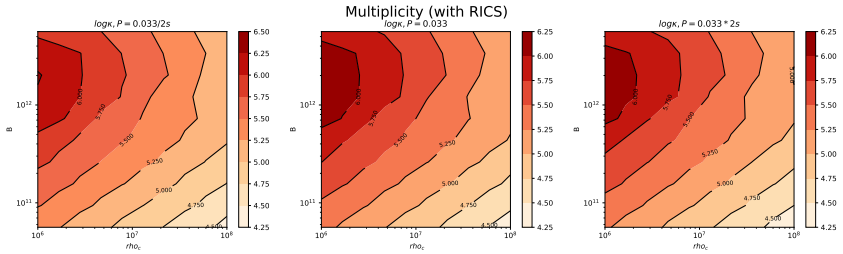

Figure 1: 在不同周期、磁场强度和磁场线曲率半径下模拟计算极冠区级联过程的粒子产率。

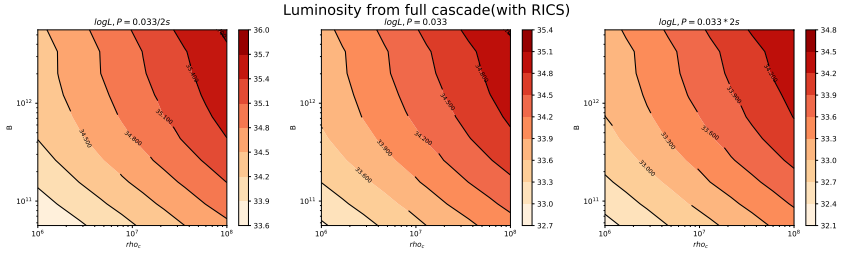

Figure 2: 在不同周期、磁场强度和磁场线曲率半径下模拟计算极冠区级联过程的脉冲星总光度。

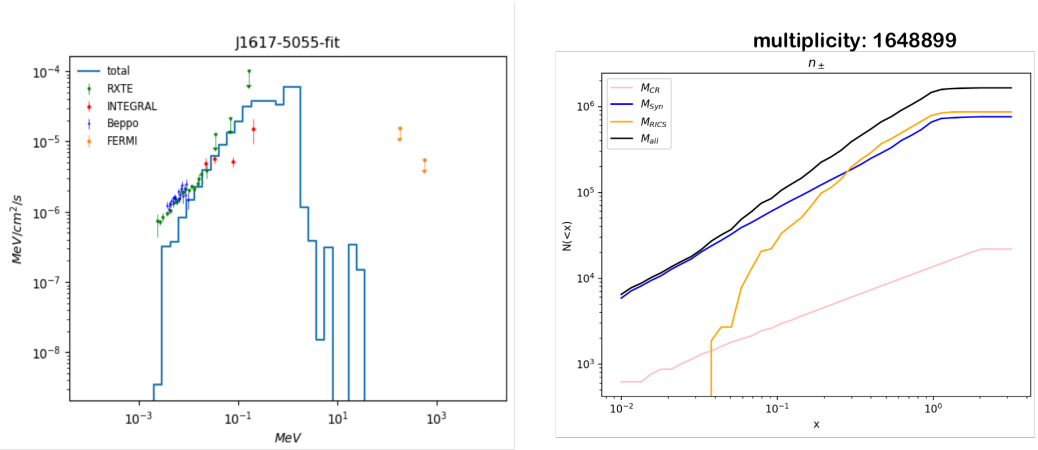

Figure 3: 左图：对PSR J1617-5055的观测进行拟合；右图：PSR J1617-5055的总产率以及各辐射过程对产率的贡献。

Scientific Program of FAST/Future Pulsar Symposium 9

August 28-30, 2020, Xiamen University, Xiamen

===== Thursday (pm), August 27 =====

4:00 -- 6:00 Registration (Xiamen Aqua Resort 厦门五缘水乡3号楼酒店前台）

===== Friday (pm), August 28 =====

1:50 Opening (Li, Ang; Fang, Taotao)

Chair: Dai, Zigao (20min = 15+5)

2:00-2:20 Huang, Yongfeng: Energy injection from the central magnetar and its effect on the GRB afterglow

2:20-2:40 Zhang, Binbin: GRB 200415A: A Short Gamma-Ray Burst from a Magnetar Giant Flare?

2:40-3:00 Lai, Xiaoyu: Merging strangeon stars: the ejecta and light curve

*3:00-3:20 Liu, Liangduan: Constraining the Long-lived Magnetar Remnants in Short Gamma-Ray Bursts from Late-time Radio Observations

*3:20-3:40 Zhang, Nai-Bo (online): GW190814's secondary component with mass (2.50 − 2.67) Msun as a super-fast pulsar

*3:40-4:00 Deng, Zhuling (online): On the Formation of PSR J1640+2224: A Neutron Star Born Massive?

Break/Coffee/Registration (4:00-4:30 pm)

Chair: Xu, Renxin (20min = 15+5)

*4:30-4:50 Men, Yunpeng: TransientX: A New High Performance Transient Search Software

*4:50-5:10 Wang, Weiyang: On the magnetospheric origin of Repeating Fast Radio Bursts

*5:10-5:30 Zhang, Yongkun: Periodic analysis of FRB121102

*5:30-5:50 Liu, Zenan: Repeating FRB from the pulsar-asteroid belt collision: frequency drifting and polarization

*5:50-6:10 Deng, Furen (online): Tianlai Dish Array Multi-Beam Forming

Dinner (6:10pm-)

===== Saturday (am), August 29 =====

Chair: Li, Di (20min = 15+5)

8:00-8:20 Luo, Jintao: Pulsar Observations and Techniques at NTSC

8:20-8:40 Pan, Zhichen: FAST Globular Cluster Pulsar Survey & High DM Millisecond Candidate

Sifting

*8:40-9:00 Kou, Feifei: Periodic and Phase-locked Modulation in PSR B1929+10 Observed with FAST

*9:00-9:20 Zhang, Lei: Pulsar Observation and Study with FAST and Parkes Radio Telescope

*9:20-9:40 Yao, Jumei: The first evidence for three-dimensional spin-velocity alignment in pulsars

*9:40-10:00 Xie, Jintao (online): The radial distribution of pulsar in Galaxy

Break Break/Coffee/Conference photo (10:00-10:30 am)

Chair: Zhu, Weiwei (20min = 15+5)

10:30-10:50 Wang, Hongguang: Pulsar Population Synthesis with the Fan Beam model

*10:50-11:10 Lu, Jiguang: Polarization and Radiation Geometry of PSR B1937+21

*11:10-11:30 Zhu, Yiyuan: Soft gamma-ray emissions from the polar cap cascade region

*11:30-11:50 Li, Hao: Software Realization of Data Processing in the Digital Terminal of Coherent Dedispersive Pulsar

*11:50-12:10 Wang, Shuangqiang (online): The two emission states of PSR B1534+12

Lunch(12:10pm-)

===== Saturday (pm), August 29 =====

Chair: Wang, Hongguang (20min = 15+5)

2:00-2:20 Shao, Lijing: New graviton mass bound from binary pulsars

*2:20-2:40 Xu, Rui: X-ray pulse profile of scalarized neutron stars in massive scalar-tensor theory of gravitation

*2:40-3:00 Miao, Xueli: Tests of Conservation Laws in Post-Newtonian Gravity with Binary Pulsars

*3:00-3:20 Gao, Yong: Triaxially-deformed Freely-precessing Neutron Stars: Continuous electromagnetic and gravitational radiation

*3:20-3:40 Liu, Mengxu: Coalescing Binary Neutron Star Systems Under a Three-Dimension Gravitational-Wave Detector

*3:40-4:00 Zhu, Zhenyu (online): Tidal deformability and gravitational-wave phase evolution of magnetised compact-star binaries

Break/Coffee (4:00-4:30 pm)

Chair: Huang, Yongfeng (20min = 15+5)

4:30-4:50 Zhang, Jie: Detecting new glitches using data from Parkes 64-m radio telescope

4:50-5:10 Dong, Jianmin: Neutron star superfluidity and cooling

*5:10-5:30 Wang, Weihua: Pulsar glitch activity in a strangeon star model

*5:30-5:50 Wu, Xuhao: What if the neutron star maximum mass is beyond ~2.3 Msun?

*5:50-6:10 Zhou, Zurong (online): Glitches detected at Nanshan and pta Simulated results

Dinner (6:10pm-)

===== Sunday (am), August 30 =====

Chair: Gong, Biping (30min = 25+5; 25min=20+5)

8:00-8:30 Dai, Zigao: 快速射电暴的起源研究

Announcement of Crab and Vela Prizes

8:50-9:15 Zhang, Shuangnan (online): SGR1935: HXMT

9:15-9:40 Lee, Kejia: SGR1935: FAST

Break/Coffee (9:40-10:10 am)

Chair: Li, Ang (20min = 15+5)

10:10-10:30 Xu, Renxin: Light-quark flavours in a triangle

10:30-10:50 Tong, Hao: Large polar caps for twisted magnetosphere of magnetars

10:50-11:10 Li, Zhaosheng: Accreting Millisecond X-ray Pulsar: X-ray outburst observations

11:10-11:30 Shang, Xinle (online): Nucleon-nucleon short-range correlations and their influence on neutron star

11:30-11:50 Hu, jinniu (online): The investigation of secondary compact object in GW190814 with DDRMF model

11:50-12:10 Xia, Chengjun (online): Supercritically charged objects and electron-positron pair creation

12:10 Closing (Li, Di)

Lunch (12:20pm-)